
Geophysical characterization of bottom simulating reflectors in the Fairway Basin (off New Caledonia, Southwest Pacific), based on high resolution seismic profiles and heat flow data

Hervé Nouzé^a, Emmanuel Cosquer^a, Julien Collot^{a, b}, Jean-Paul Foucher^a, Frauke Klingelhoefer^a, Yves Lafoy^b and Louis Géli^{a, *}

^a Ifremer, Marine Geosciences Department, BP 70, 29280, Plouzané, France

^b Geological Survey of New Caledonia, Department of Industry, Mines and Energy of New Caledonia, BP 465, 98845 Nouméa cedex, New Caledonia

*: Corresponding author : L. Géli, email address : geli@ifremer.fr

Abstract:

High-resolution reflection and refraction seismic data were collected in 2004 to investigate, in further detail than allowed by pre-existing low resolution seismic data, the nature of a Bottom Simulating Reflector (BSR) that extends over a broad area of the Fairway Basin, a rifted, continental structure located on the eastern flank of the Lord Howe Rise, to the southwest of New Caledonia. Two main reflectors are documented: the shallower (RN) mimics the seafloor and has a negative polarity while the deeper (RP) does not always mimic the seafloor and has a positive polarity. Using the existing regional seismic lines, we can show that reflector RN can be continuously followed up to DSDP 208 drill hole site. Reflector RP is discontinuous and cannot be traced to DSDP 208. Based on DSDP 208 stratigraphic data, Reflector RN is assigned to the Eocene/Oligocene regional unconformity; reflector RP is interpreted in terms of a diagenetic BSR, likely related to an Opal-A/Opal-CT transition front. Heat flow data collected in 2006 suggest that reflector RP lies too deep to be related to methane hydrates, strengthening our interpretation that RP is of diagenetic origin.

Keywords: BSR; Fairway Basin; Southwest Pacific; geophysics; gas hydrates; stratigraphy

1. Introduction

Following R/V "Rig Seismic" AGSO Surveys 177 (e.g. Ramsay et al., 1997) and 206 (e.g. [Lafoy et al., 1998] and [Bernardel, 1999]), a Bottom Simulating Reflector (BSR) was identified (Fig. 1 and Fig. 2) in the southernmost part of the Central Fairway Basin (Exon et al., 1998). This BSR was later shown, from ZoNeCo 5 cruise data (Auzende et al., 2000a J.-M. Auzende, S. Van de Beuque, G. Dickens, C. François, Y. Lafoy, O. Voutay and N. Exon, Deep sea diapirs and bottom simulating reflector in Fairway basin (SW Pacific), Marine Geophysical Researches 21 (2000), pp. 579–587. Full Text via CrossRef | View Record in Scopus | Cited By in Scopus (10)Auzende et al., 2000a), to extend further north in the Central Fairway Basin, over an area of several tens of thousands of km² located in the offshore domain of New Caledonia (Auzende et al., 2000a). The BSR lies at a depth of 500–600 m. It was described as clearly

36 cross-cutting sedimentary strata, but of small amplitude and with a positive polarity.

37

38 For a general review, refer to Exon et al. (2007). Based on previous work by Exon et al. (2004a),
39 Pecher (2004) and Nouzé et al. (2005), it is proposed that the BSR in the Fairway could result from:
40 1) a diagenetic phase transformation; 2) a thin gas layer with a sharp top; or 3) the sharp base of a
41 gas layer (probably beneath gas hydrates) of thermogenic origin. As part of the ZoNeCo-11 cruise
42 of R/V L'Atalante in 2004, further seismic field work was carried out in the Fairway basin (Figure 1)
43 to investigate the BSR distribution and its properties in considerably greater detail than allowed by
44 previously collected low resolution seismic data (ZoNeCo 5). Four 2D high resolution reflection
45 seismic lines (Z11-11 to Z11-14) were shot and recorded on 12 Ocean Bottom Seismometers
46 (OBS). The seismic study was further complemented by heat flow measurements taken at five
47 distinct sites of the Fairway Basin with R/V Marion Dufresne during the ZoNeCo-12/Ausfair cruise
48 (Foucher and scientific party, 2006). Here, we present these newly acquired seismic and heat flow
49 data and discuss the nature of the BSR in the Fairway Basin.

50

51 **2. Regional geological context**

52

53 The Fairway Basin is located between Australia and New Caledonia. It extends over about 800 km
54 in a NNW-SSE direction. It is ~ 120-200 km wide, limited to the SW by the Lord Howe Rise and
55 separated from the New Caledonia basin by the Fairway Ridge to the NE (Figure 1). In the Fairway
56 Basin, seafloor depth increases southwards, from ~ 1500 m to ~3000 m, as well as the sedimentary
57 thickness - from about 2000 m in the North Fairway Basin, up to 4000m in the South Fairway Basin
58 (e.g. Auzende et al., 2000a; 2000b).

59

60 The Fairway Basin was interpreted until recently (e.g. Ravenne et al., 1977; Lafoy et al., 1994), as
61 an oceanic basin resulting from the fragmentation of the eastern Gondwana during the Late
62 Cretaceous and Early Palaeogene (82-52 Ma) (e.g. Weissel and Hayes, 1972; Hayes Dennis and
63 Ringis, 1973; Gaina et al., 1998). Based on new refraction and reflection seismic data, it is now
64 proposed that it has developed on a thinned continental crust (Lafoy et al., 2005; Klingelhoefer et
65 al., 2007).

66

67 Using previous seismic surveys (Van de Beuque et al., 1998, 2003; Auzende et al., 2000c; Exon et
68 al., 2004b) and DSDP drilling (e.g. Burns et al., 1973d; 1973b), Exon et al. (2007) have proposed a
69 regional stratigraphy comprising three main sedimentary units. Upper Cretaceous and pre-Upper
70 Cretaceous sequences (Unit 3) appear on seismic sections as a poorly bedded unit, resting on the

71 basement. They are overlain by Paleocene and Eocene chalks and radiolarites with cherts (Unit 2)
72 that correspond to a well-bedded seismic unit up to 1500 m thick. Upper Oligocene to Middle
73 Miocene chalks, and Middle Miocene to recent calcareous oozes (Unit 1) form the upper, more
74 transparent seismic unit that is 500 to 600 m thick in our study area. Two major, regional
75 unconformities delimit these three major seismic units, respectively: the mid-Paleocene/Lower
76 Eocene unconformity and the Upper Eocene/Lower Oligocene unconformity. Figure 3 synthesises
77 the geological data available from DSDP well sites 206, 207 and 208.

78

79 Diapirs were reported in the Fairway Basin (Auzende et al., 2000a; 2000c; Van de Beuque, 2003).
80 These are circular features, ~ 3 to 15 km wide, or form elongated ridges up to 50 km long. They do
81 not appear to pierce through the seabed but some reach shallow sub-bottom depths. Diapiric
82 material appears to arise from the basal sedimentary layer of the basin, presumably made of Upper
83 Cretaceous sediments. The nature of this layer remains however debated. Diapirs could be salt
84 diapirs or mud diapirs as the area was not favourable to salt deposition during Cretaceous times.
85 Other larger diapir-like features could well be of volcanic origin (Lafay et al., 1994; Exon et al.,
86 2007).

87

88 **3. High-Resolution seismic data: acquisition and processing details**

89

90 The surface seismic acquisition system was set up to acquire high resolution data (Figure 1). It uses
91 a 3.3 km long streamer composed of 264 live channels, with a 12.5m group interval and towed at 3m
92 immersion. The data were sampled at 1ms, and recorded using a SEAL lab. The source was
93 composed of an array of 2 G-I guns and 3 mini G-I, with a total volume of 396 inch³. It was
94 operated at a nominal pressure of 140 bars, and immersion was set between 2.0 and 3.0 m in order
95 to increase the high frequency content of the recorded signal, which was centered on 90 Hz.
96 Shooting interval was 25 m, resulting in a maximum fold of 66. The processing sequence applied
97 to the high resolution seismic reflection data comprised: 1) SegD data input ; 2) geometry and CDP
98 binning ; 3) shooting delay correction ; 4) frequency band pass filtering (15-230 Hz) ; 5) Spherical
99 divergence corrections (water velocity) ; 6) velocity analysis ; 7) Normal Move Out corrections ; 8)
100 CDP stacking ; 9) Poststack time migration with a smoothed velocity model. These 4 profiles show
101 good quality data (Figure 4 and 5). Penetration observed on processed data reaches about 2 s two
102 way timetravel (twl) (except when crossing the ridge) and vertical resolution is better than 10 m.

103

104 The seismic signal was also recorded on 12 OBSs, that were deployed in 3 clusters, each cluster
105 being composed of three OBSs deployed about 500 m apart from each other along the main

106 shooting line (Z11-11) and one OBS offset by about 1 km in a direction perpendicular to the main
107 shooting line. This acquisition scheme was designed to investigate the subsurface at 3 sites
108 distinguished by their location with respect to the dome that affects the basement near the
109 intersection between lines Z11-11 and Z11-12: Site 1 is located away from the basement dome; Site
110 2 is on its flank; and Site 3 at its apex. OBS data was recorded at 1 ms sampling rate. The
111 processing sequence applied to the OBS records is summarised as follows: 1) shot time quality
112 control and corrections (instrument skew, shooting delay, instrument recording delay); 2) data
113 conversion to SegY format; 3) frequency band pass filtering (15-230 Hz); 4) picking of direct
114 arrival times; 5) re-positioning (X, Y, Z) of OBS and determination of a best-fitting water velocity
115 from the inversion of first arrival times; 6) spherical divergence corrections. The vertical resolution
116 of the OBS hydrophone data, reported in this paper, is better than 10 m, and thanks to a low noise
117 level on the instruments, sediment penetration reaches 2s twt.

118

119 **4. Analysis of ZoNeCo-11 high resolution seismic data**

120

121 Seismic line Z11-11 is centered on a basement dome, about 5 km wide (Figure 4). The basement
122 reflector that delimits the dome appears to extend laterally to deep events marked as B on both sides
123 of the dome. From the basement (above B events) to the seabed, the three main sedimentary units
124 that have been proposed by Exon et al. (2007) are recognized :

125

- 126 ➤ Unit 3, about 300 ms thick at Site 1 (OBS 03), shows low amplitude, discontinuous
127 reflectors. This unit disappears near the dome.
- 128 ➤ Unit 2 is composed of continuous, sub parallel strata. It is separated from Unit 3,
129 underneath, by a strong positive polarity reflector, C. The top of the layer is marked by a
130 reflector, hereafter named RN, of strong amplitude and negative polarity. A strong reflector
131 with positive polarity, RP, cuts across the strata of Unit 2. Away from the dome, RP is
132 slightly chaotic. On the flanks, RP deepens, clearly cross cuts stratigraphic horizons, and
133 sometimes coincides with these stratigraphic horizons for a short distance (Figure 4 and 5).
134 RP is associated with a change in reflectivity, especially visible on the flanks of the
135 intrusion, where reflectivity amplitudes are attenuated and frequency spectra are altered
136 below RP with respect to the strata above.
- 137 ➤ Unit 1 appears as poorly reflective and affected by numerous sub-vertical faults (examples
138 marked by F on Figure 4 and 5).

139

140 Reflectors RN and RP were further characterized using OBS data. Arrival times were 2D-inverted

141 into velocity profiles using RAYINV software of Zelt and Smith (1992). In order to pick the arrival
142 times more easily, the seabed on OBS gathers was “flattened” using the re-positioned source and
143 receiver locations and the best-fitting water velocity to calculate a direct arrival time that was
144 subsequently subtracted from the arrival times for this configuration. Sediment velocity resolution
145 ranges from about 25 m/s for shallow layers to about 80 m/s for deep layers. Then, the OBS
146 reflectors were correlated with HR seismic line reflectors (RN and RP on Figure 6b). The results
147 clearly indicate that the P-wave velocity decreases with depth across RN, while it increases across
148 RP (Figure 6b).

149

150 **5. DSDP stratigraphy.**

151

152 DSDP Site 208 on the Lord Howe Rise is of particular interest to this study because the stratigraphy
153 revealed by the drilling data can be seismically tied up to the Fairway Basin (Figure 2). Drilling
154 penetrated 320 m of recent foraminifera-bearing to Middle Miocene nannofossil oozes, then about
155 170 m of Middle Miocene to Middle Eocene nannofossil chalks (e.g. Burns et al., 1973d; Kennett et
156 al., 1986). At 488 m below the seabed, the drilling reached the Eocene/Oligocene unconformity
157 (Figure 3). Below the unconformity, siliceous sediments (radiolaria, diatoms, sponge spicules,
158 silicoflagellata) were recovered, the matrix being composed of calcium carbonate. P-wave
159 velocities and sediment densities at Site 208 decrease with depth across the Eocene / Oligocene
160 unconformity because of the occurrence of siliceous sediments of increased sediment porosity
161 (Burns et al., 1973a; 1973d). The oldest sediments drilled at DSDP Site 208 are Upper Cretaceous
162 marine silico-clastic sediments.

163

164 Site 206 in the South New Caledonia Basin, penetrated the same sedimentary sequence (Figure 3).
165 The Eocene / Oligocene unconformity was reached at 614 m below the seabed and the same P-wave
166 velocity and density inversions were observed across this unconformity. Drilling data thus confirms
167 the regional extent of the sedimentary units and unconformities.

168

169 **6. Linking DSDP Site 208 to the Fairway Basin: Regional Significance of RN and RP**

170

171 **6.1 Reflector RN**

172 To correlate the stratigraphic information from DSDP Site 208 to the reflectors documented in the
173 Fairway Basin, we used the multichannel seismic lines collected during AGSO/Surveys 206 and
174 177 of R/V Rig Seismic (Figure 2) and all the 6-channel seismic lines that were collected in 1999
175 during the ZoNeCo-5 cruise of R/V L'Atalante and recently reprocessed for the purpose of the

176 present work. See Appendix 1 in supplementary electronic data for more details on the correlation
177 of seismic line s206-2 (FAUST-1 survey - (Lafoy et al., 1998) to DSDP 208 drill site (Burns et al.,
178 1973d). At DSDP Site 208, a correspondence was established between the Eocene/Oligocene
179 Unconformity (EOU) and a reflector documented on seismic line FAUST1-S206-2, which exhibits
180 two remarkable characteristics: 1) it corresponds to a seismic phase inversion; 2) it separates a
181 transparent layer with only one intra-Miocene reflector above, from a layer with numerous, well
182 bedded sequences. This reflector, now associated to the EOU, can be tracked from the drill hole
183 continuously to the Fairway Basin, following 2 different paths (Figure 2):

184

185 ➤ The northern path (Collot et al., 2008) : from DSDP Site 208 along line Faust1-S206-2 up
186 to the intersection with FAUST1-S206-1 ; then along this line up to the crest and down to
187 the eastern flank of Lord Howe Rise, where a reflector related to a seismic phase inversion
188 is found at the base of a seismically transparent layer. The link to our study area in the
189 Fairway Basin is then provided by seismic profiles ZoNeCo11-11, -10 and -09.

190

191 ➤ The southern path: from DSDP Site 208 to the intersection with FAUST1-S206-3; then
192 along this line up to the crest and down to the eastern flank of Lord Howe Rise (the
193 identification in the basin is based on the same criteria as above : strong reflector with
194 negative polarity at the base of a transparent layer) until line S 177- LHRNR-BA. This
195 profile is very interesting because it is crosscut by numerous ZoNeCo5 profiles. The EOU
196 was identified on all these crosscutting ZoNeCo5 profiles. Then, the link to our study area
197 was provided by the ZoNeCo5-07 line (Figure 7) that connects to ZoNeCo-11 lines 09, 10
198 and 11.

199

200 In both cases, a clear correspondence is found between the EOU and reflector RN in the Fairway
201 Basin.

202

203 In summary, RN: (1) has a negative polarity, (2) mimics approximately the sea floor but (3) does
204 not cross-cut the sedimentary layers, (4) corresponds to the Eocene/Oligocene unconformity drilled
205 at DSDP Site 208.

206

207 **6.2 Reflector RP**

208 Reflector RP, described above in section 4, is discontinuous and cannot be traced from the Fairway
209 Basin to DSDP site 208. The BSR reflector that was identified by Auzende et al. (2000a) on the
210 seismic lines collected during the ZoNeCo5 cruise, corresponds to RP (Figure 7 and 8). It is

211 important to note that RP lies always below the Eocene/Oligocene Unconformity.
212 In summary, RP: (1) has a positive polarity (2) does not always mimic the sea floor (3) clearly
213 cross-cuts sedimentary layers, (4) is always situated deeper than the Eocene/Oligocene
214 unconformity (RN), (5) corresponds to the BSR previously described by Auzende et al. (2000a)
215 from ZoNeCo 5 seismic data.

216

217 **7. Heat flow constraints**

218

219 Heat flow data (Figure 9 and Table 1) were collected at 5 different sites in the study area in
220 February 2006 with R/V Marion Dufresne (Foucher and scientific party, 2006). Sediment
221 temperature at each site was measured at up to 7 different depths in the sub-bottom by means of
222 thermistor temperature sensors attached on outriggers to a 18 m long lance of the CALYPSO
223 gravity corer of the R/V Marion Dufresne. Sediment equilibrium temperatures were extrapolated
224 from thermal transients recorded for 6-10 mn following penetration. Thermal conductivity was
225 measured by the needle probe technique on the recovered core at each heat flow measurement site.
226 The relative accuracy of temperature measurements is estimated to be better than 0.01 °C (for each
227 temperature sensor with respect to other sensors) and 5% for conductivity measured on cores.

228

229 Two sites (MD06-3022 and MD06-3023) are located along seismic profile ZoNeCo11-11. At the
230 apex of the basement high (site MD06-3022), the measured heat flux is 54 mW/m². Less than 2.5
231 km away to the south (site MD06-3023), the heat flux is 49 mW/m². The three remaining sites are
232 located along seismic profile ZoNeCo11-09. At these sites, the layer above the Eocene-Oligocene
233 Unconformity appears to be crosscut by normal faults along which fluid escapes are suspected. Heat
234 flux was measured to be 64, 53 and 49 mW/m² at sites MD06-3026, 3027 and 3028 respectively.

235

236 The above heat flow data provide the first available information on the thermal regime of the
237 Fairway Basin. The heat flow values are fairly consistent, ranging from 49 to 64 mW/m². The
238 spatial variability could be explained by heat flow refraction or fluid flow effects. The higher heat
239 flow of 54 mW/m² at the apex of the basement ridge at site MD06-3022, with respect to the slightly
240 lower value of 49 mW/m² measured at site MD06-3023 on the flank of this ridge, could be a result
241 of heat flow refraction from low thermal conductivity sediments surrounding the ridge to the higher
242 thermal conductivity body that the ridge is likely to be. On the other hand, the variable heat flow
243 values of 49-64 mW/m² at sites MD06-3026, 3027 and 3028 may indicate disturbances to the
244 conductive thermal regime due to fluid advection along normal faults observed on the seismic
245 section Z11-09.

246

247 Based on these data, the gas hydrate z-T stability field was calculated using the method described in
248 Sultan et al. (2004). Thermal conductivity was measured on cores taken at heat flow stations.
249 Measurements indicate a value of $\sim 1.0 \text{ WK}^{-1}\text{m}^{-1}$ at seabed. For deeper sediments, thermal
250 conductivity was estimated from:

$$251 \quad \lambda = \lambda_w^{(1-\phi)} \cdot \lambda_m^\phi$$

252 where λ_w is the thermal conductivity of water ($0.7 \text{ WK}^{-1}\text{m}^{-1}$), λ_m is the thermal conductivity of the
253 sediment matrix and ϕ is the porosity. DSDP Sites 206, 207 and 208 data showed an upper
254 sedimentary sequence made of calcareous ooze, from Oligocene to Recent, above the Eocene-
255 Oligocene unconformity, and a mean porosity of 60%. Taking $\lambda_m = 3.0 \text{ WK}^{-1}\text{m}^{-1}$, a conventional
256 value for calcite, and $\phi = 0.6$, an estimated value of the thermal conductivity, λ , is $1.25 \text{ WK}^{-1}\text{m}^{-1}$.
257 Allowing for some uncertainty in this value and its distribution with depth, the thermal conductivity
258 was assumed to be constant with depth and ascribed to vary between 1.0 and $1.5 \text{ WK}^{-1}\text{m}^{-1}$. We have
259 also assumed that: 1) heat transfer in the sediment column is purely conductive; 2) sediment pore
260 water salinity is constant and equal to $\sim 34.9 \text{ ‰}$ (Jean-Luc Charlou, pers. comm. 2008); 3) hydrate
261 is from methane gas only. The depths of the base of the gas hydrate stability zone (GHSZ) at each
262 heat flow measurement site was computed using the HYSFA Code (Sultan et al., 2004). Results are
263 listed in Table 2. At all sites, except for MD06-2328, reflector RP lies deeper than what is
264 considered to be an acceptable range for the base of the methane gas hydrate stability zone. Heat
265 flow data alone cannot be considered as a proof per se, as other sources of uncertainties - such as
266 gas composition or depth determination - may occur. If the clathrate gas were made of hydrocarbon
267 gases heavier than methane, the theoretical BSR could lie deeper than expected. Also, errors in
268 depth conversion cannot be ruled out, however the quality of the high resolution data that we use
269 and the availability of velocity determinations based on OBSs (Figure 6) are such that uncertainties
270 appear unlikely to significantly alter our conclusions.

271

272 **8. Discussion: nature of the BSR in the Fairway Basin**

273

274 Here, we discuss the different hypotheses retained by Exxon et al. (2007) to explain the occurrence
275 of the BSR (our RP reflector), mainly: gas or gas hydrate versus diagenetic front. A BSR at the top
276 of a gas hydrate layer has been observed on the Nankai margin, offshore Japan (Nouze et al., 2004),
277 where coarse sediment layers contain large amounts of gas hydrate (up to 70-80% of the pore
278 space). As illustrated by this example, a significant content of hydrate is necessary to create an
279 impedance contrast strong enough to generate a clear reflector associated with the presence of
280 hydrate, and thus a significant amount of gas is required in the sediment to form this hydrate. The

281 BSR in the Fairway Basin is present extensively (Auzende et al., 2000a), but there has been so far
282 no evidence of a high content of potentially-hydrate-forming gas (hydrocarbons) in cores taken in
283 the Fairway Basin along ZoNeCo-11 study site (Jean-Luc Charlou, personal communication).
284 Furthermore, should the top of a gas hydrate layer be detected by a BSR, one would expect its
285 bottom to be observed as well, as this is the case in the Nankai margin (e.g. Nouze et al., 2004).
286 Another strong argument against the hydrate-related BSR hypothesis arises from the heat flow
287 results presented in this paper. If hydrate occurrences in the Fairway Basin were to be dominated by
288 methane hydrate, the BSR would lie too deep below the seabed to lie in the stability field of a
289 methane hydrate. Moreover, the large lateral extent of the BSR within the Fairway Basin over more
290 than 70,000 km², mapped with the ZoNeCo-5 survey by Auzende et al. (2000a), is unusual for gas-
291 hydrate BSR and much more typical for opal A / CT BSR. Note that Exon et al. (2004a; 2007)
292 identified a similar BSR farther south (around 31°S) in the southern Fairway Basin, located on the
293 flanks of the East Lord Howe Spur (profiles 10 and 11 of seismic survey s232). This further
294 confirms the regional extent of the BSR and reinforces the argument of a non-gas-hydrate related
295 BSR.

296

297 On the other hand, Exon et al. (2007) considered that if the BSR were of diagenetic origin, « it
298 could only have been generated by an upward moving, silica-rich diagenetic front ». These authors
299 rejected the hypothesis of an Opal-A / Opal-CT transition because, according to their interpretation,
300 the BSR would lie above the Eocene/Oligocene unconformity, hence in carbonates almost devoid of
301 silica according to DSDP Site 208 data. Our interpretation for the position of the Eocene/Oligocene
302 unconformity in the Fairway Basin differs from that proposed by Exon et al. (2007). We have
303 shown that the BSR indeed lies within Eocene siliceous sediments. Thus the major argument against
304 the hypothesis no longer holds. On the contrary, the recovery in mid-Eocene sediments at DSDP
305 Site 208 of a piece of porcelanite, made from cristobalite (i.e. Opal-CT) resulting from re-
306 crystallisation of biogenic silica, gives support to the interpretation of the BSR as an impedance
307 contrast at the Opal-A / Opal-CT transition.

308

309 The Opal-A / Opal-CT transition has been widely discussed in the literature. Opal-A, which was
310 defined by Jones and Segnit (1971), is a siliceous ooze resulting from the dissolution of siliceous
311 organisms tests. With the burying with sediments, pressure and temperature increase and a
312 dissolution re-precipitation reaction converts opal-A into opal-CT. This reaction generates an
313 interface between the two types of opal with an increase in density and a decrease in porosity and
314 permeability, involving an impedance contrast strong enough to create a reflector with positive
315 polarity (e.g. Ramsay, 1971; Hempel et al., 1989; Lee et al., 2003). Temperature is a main parameter

316 controlling the Opal-A / Opal-CT transition. However, this diagenetic process is also influenced by
317 pressure, time (related to the burying of the siliceous sediments), nature of the surrounding rocks
318 (e.g. carbonates increase the reaction rate), and interstitial waters (e.g. Hein et al., 1978; Williams
319 and Crerar, 1985; Kuramoto et al., 1992; Nobes et al., 1992; Davies, 2005). BSRs have been
320 interpreted as an opal-A / opal-CT transformation in several areas of the world including Monterey
321 Formation in California (Isaacs, 1982), Bermuda Rise (Thein and von Rad, 1987), the Antarctic
322 basin (Botz and Bohrmann, 1991), the Japan Sea (Kuramoto et al., 1992), the Norwegian Sea
323 (Henrich, 1989; Berndt, 2004), the Faeroe-Shetland basin (Davies and Cartwright, 2002), New
324 Zealand (Lynne and Campbell, 2004), the Southwest Indian ridge (Gerland et al., 1997). Volpi et al.
325 (2003) reported observations of a diagenetic BSR related to the Opal-A/Opal-CT transformation on
326 the Pacific margin of the Antarctic Peninsula. The BSR clearly crosscuts the stratigraphy and
327 divides the sedimentary layer into a strong reflectivity zone (above) and a low reflectivity zone
328 (below) (Figure 10b). One will note that this change in reflectivity across the BSR at the Antarctic
329 site shares strong similarities with our own observations on ZoNeCo-11 seismic profiles (Figure
330 10a). Also, as noted by Volpi et al. (2003), the diagenetic alteration of opal-A to opal-CT causes a
331 dramatic reduction of intra- and interskeletal porosity, resulting in overpressuring in altered
332 sediments and settlement of channelised fluid escape features from these sediments to the seabed.
333 Davies and Cartwright (2002) estimated that the volume reduction associated with the Opal-A /
334 Opal-CT transformation could be 30–40%, an amount large enough to account for the
335 development of a polygonal fault system. Such a fault system may have \square rench \square ia within the
336 sedimentary layers above the BSR in the Fairway Basin as suggested by the complex network of
337 small-offset vertical faults visible on our 2D seismic lines (Figure 4 and 5). All these observations
338 favour an interpretation of the BSR in the Fairway Basin as related to an Opal-A / Opal-CT
339 transition. Finally, on ZoNeCo-11 line Z11-11, the BSR appears to deepen on the flanks of the
340 basement dome with respect to a bump in the sedimentary layers (Figure 5). A downward shift in
341 the Opal A – Opal CT transition could result from a pressure decrease due to faulting or a
342 temperature distribution altered by the formation of the basement dome.

343

344 **9. Conclusion**

345

346 The present work sheds light on the stratigraphy of the Fairway Basin as well as the nature of its
347 BSR. Two major reflectors, RN and RP, were identified on the high-resolution lines, and correlated
348 to DSDP drilling data. RN is a negative polarity reflector, mimicking approximately the seafloor.
349 According to our interpretation, RN is a regional reflector that marks the Eocene/Oligocene
350 unconformity. The negative polarity of RN is accounted for by low V_p velocity and density of

351 silica-rich Eocene sediments with respect to overlying Oligocene carbonate oozes. RP is a positive
352 polarity reflector, crosscutting sediment strata. Both seismic and heat flow data tend to support the
353 interpretation of this reflector as a diagenetic front (Opal-A / opal-CT transition) rather than a
354 methane-hydrate BSR.

355

356 **Acknowledgments :**

357

358 The ZoNéco-11 and ZoNéCo-12 cruises were conducted within the framework of the
359 ZoNéCo program (Assessment of living and non-living resources of New Caledonia
360 EEZ) funded by ADECAL (Agency for the Economic development of New Caledonia).
361 We thank the following people and organizations: IFREMER, IPEV and the Service
362 Géologique de Nouvelle-Calédonie ; shipboard party of cruises ZoNéCo-11 and
363 ZoNéCo-12 cruises ; officers and crew of R/V l'Atalante and R/V Marion Dufresne. We
364 are also grateful to G. Bernardel from Geoscience Australia (former AGSO) for the co-
365 owned FAUST data New Caledonia / Australia. Special thanks to Nabil Sultan for
366 providing the HYSFA Code; to Yvon Balut (IPEV) ; to François Harmegnies for
367 collecting the heat flow data and to Jean-Luc Charlou for communicating unpublished
368 data collected during the ZoNéco-12 Cruise. Maps are produced with the Generic
369 Mapping Tool 4.2.1 (<http://gmt.soest.hawaii.edu>), seismic data was processed with
370 CGG-Geocluster and IFREMER-Sisbise.

372 **References**

- 373 Auzende, J.-M., Van de Beuque, S., Dickens, G., François, C., Lafoy, Y., Voutay, O., Exon, N.,
 374 2000a. Deep sea diapirs and bottom simulating reflector in Fairway basin (SW Pacific).
 375 *Marine Geophysical Researches* 21, 579-587.
- 376 Auzende, J.-M., Van de Beuque, S., Regnier, M., Lafoy, Y., Symonds, P., 2000b. Origin of the New
 377 Caledonian ophiolites based on a French-Australian Seismic Transect. *Marine Geology*
 378 162(2-4), 225-236.
- 379 Auzende, J.M., Beneton, G., Dickens, G., Exon, N., Francois, C., Hodway, D., Juffroy, F., Lafoy, Y.,
 380 Leroy, A., van de Beuque, S., Voutay, O., 2000c. Mise en évidence de diapirs mésozoïques
 381 sur la bordure orientale de la ride de Lord Howe (Sud-Ouest Pacifique) : campagne ZoNeCo
 382 5. *Comptes rendus de l'Académie des sciences, Série II, Sciences de la terre et des planètes*
 383 330(3), 209-215.
- 384 Bernardel, G., 1999. Preliminary results from AGSO Law of the Sea Cruise 206: an
 385 Australian/French collaborative deep seismic marine survey in the Lord Howe Rise/New
 386 Caledonia region. Australian Geological Survey Organisation record 1994/14, 37.
- 387 Berndt, C.B., S.; Clayton, T.; Mienert, J.; Saunders, M., 2004. Seismic character of bottom simulating
 388 reflectors: examples from mid-Norwegian margin. *Marine and Petroleum Geology* 21, 723-
 389 733.
- 390 Botz, R., Bohrmann, G., 1991. LOW-TEMPERATURE OPAL-CT PRECIPITATION IN
 391 ANTARCTIC DEEP-SEA SEDIMENTS - EVIDENCE FROM OXYGEN ISOTOPES.
 392 *Earth and Planetary Science Letters* 107(3-4), 612-617.
- 393 Burns, R.E., Andrews, J.E., Van der Lingen, G.J., Andrews, J.E., Churkin, M., Jr., Davies, T.A.,
 394 Dumitrica, P., Edwards, A.R., Galehouse, J.S., Kennett, J.P., Packham, G.H., 1973a.
 395 Regional aspects of deep sea drilling in the Southwest Pacific, Lithostratigraphy of Eight
 396 Drill Sites in the South-west Pacific. Preliminary Results of the Deep Sea Drilling Project
 397 21.
- 398 Burns, R.E., Andrews, J.E., van der Lingen, G.J., Churkin, M., Jr., Galehouse, J.S., Packham, G.,
 399 Davies, T.A., Kennett, J.P., Dumitrica, P., Edwards, A.R., Von Herzen, R.P., 1973b. Site 206.
 400 Initial Reports of the Deep Sea Drilling Project - Leg 21(Suva, Fiji to Darwin, Australia
 401 Nov. 1971-Jan. 1972), 103-195.
- 402 Burns, R.E., Andrews, J.E., van der Lingen, G.J., Churkin, M., Jr., Galehouse, J.S., Packham, G.,
 403 Davies, T.A., Kennett, J.P., Dumitrica, P., Edwards, A.R., Von Herzen, R.P., 1973c. Site 207.
 404 Initial Reports of the Deep Sea Drilling Project - Leg 21(Suva, Fiji to Darwin, Australia
 405 Nov. 1971-Jan. 1972), 197-269.
- 406 Burns, R.E., Andrews, J.E., van der Lingen, G.J., Churkin, M., Jr., Galehouse, J.S., Packham, G.,
 407 Davies, T.A., Kennett, J.P., Dumitrica, P., Edwards, A.R., Von Herzen, R.P., 1973d. Site 208.
 408 Initial Reports of the Deep Sea Drilling Project - Leg 21(Suva, Fiji to Darwin, Australia
 409 Nov. 1971-Jan. 1972), 271-331.
- 410 Collot, J., Géli, L., Lafoy, Y., Vially, R., Cluzel, D., Klingelhoefer, F., Nouzé, H., 2008. Tectonic
 411 history of northern New Caledonia Basin from deep offshore seismic reflection: Relation to
 412 late Eocene obduction in New Caledonia, southwest Pacific. *Tectonics* 27(TC6006),
 413 doi:10.1029/2008TC02263.
- 414 Davies, R.J., 2005. Differential compaction and subsidence in sedimentary basins due to silica
 415 diagenesis: A case study. *Geological Society of America Bulletin* 117(9-10), 1146-1155.
- 416 Davies, R.J., Cartwright, J., 2002. A fossilized Opal A to Opal C/T transformation on the northeast
 417 Atlantic margin: support for a significantly elevated Palaeogeothermal gradient during the
 418 Neogene? *Basin Research* 14(4), 467-486.
- 419 Exon, N., Dickens, G., Auzende, J.-M., Lafoy, Y., Symonds, P., van de Beuque, S., 1998. Gaz
 420 hydrates and free gas on the Lord Howe Rise, Tasman Sea. *Petroleum Exploration Society
 421 of Australia Journal* 26, 148-158.

- 422 Exon, N., Hill, P., Lafoy, Y., Fellows, M., Perry, K., Mitts, P., Howe, R., Chaproniere, G.C.H.,
423 Dickens, G., Ussler, B., Paull, C.K., 2004a. Geology of the Fairway and New Caledonia
424 basins in the Tasman Sea: sediment, pore water, diapirs and bottom simulating reflectors
425 (Franklin cruise FR9/01 and Geoscience Australia Survey 232). Geoscience Australia
426 Record 2004(26), 1-112.
- 427 Exon, N., Lafoy, Y., Hill, P.J., Dickens, G., Pecher, I., 2007. Geology and petroleum potential of the
428 Fairway Basin in the Tasman Sea. Australian Journal of Earth Sciences 54, 629-645.
- 429 Exon, N., Quilty, P., Lafoy, Y., Crawford, A.J., Auzende, J.-M., 2004b. Miocene volcanic seamounts
430 on northern Lord Howe Rise: lithology, age and origin. Australian Journal of Earth Sciences
431 51, 291-300.
- 432 Foucher, J.P., Scient.party, 2006. Rapport de la campagne AUSFAIR/ZoNéCo-12, à bord du N/O
433 Marion Dufresnes. 12-26 Février 2006.
- 434 Gaina, C., Mueller, D.R., Royer, J.-Y., Stock, J., Hardebeck, J.L., Symonds, P., 1998. The tectonic
435 history of the Tasman Sea: a puzzle with 13 pieces. Journal of Geophysical Research - Solid
436 Earth 103(6), 12,413-12,433.
- 437 Gerland, S., Kuhn, G., Bohrmann, G., 1997. Physical properties of a porcellanite layer (Southwest
438 Indian Ridge) constrained by geophysical logging. Marine Geology 140(3-4), 415-426.
- 439 Hayes Dennis, E., Ringis, J., 1973. Seafloor Spreading in the Tasman Sea. Nature (London)
440 244(5408), 454-458.
- 441 Hein, J.R., Scholl, D.W., Barron, J.A., Jones, M.G., Miller, J., 1978. DIAGENESIS OF LATE
442 CENOZOIC DIATOMACEOUS DEPOSITS AND FORMATION OF BOTTOM
443 SIMULATING REFLECTOR IN SOUTHERN BERING SEA. Sedimentology 25(2), 155-
444 181.
- 445 Hempel, P., Mayer, L., Taylor, E., Bohrmann, G., Pittenger, A., 1989. The influence of biogenic
446 silica on seismic lithostratigraphy at ODP sites 641 and 643, Eastern Norwegian Sea.
447 Proceedings of the Ocean Drilling Program, Scientific Results, 104.
- 448 Henrich, R., 1989. Diagenetic environments of authigenic carbonates and opalCT crystallization in
449 lower Miocene to upper Oligocene deposits of the Norwegian Sea (ODP Site 643, Leg 104).
450 Proceedings of the Ocean Drilling Program, Scientific Results, 104.
- 451 Isaacs, C.M., 1982. INFLUENCE OF ROCK COMPOSITION ON KINETICS OF SILICA
452 PHASE-CHANGES IN THE MONTEREY FORMATION, SANTA-BARBARA AREA,
453 CALIFORNIA. Geology 10(6), 304-308.
- 454 Jones, J.B., Segnit, E.R., 1971. The nature of Opal I. Nomenclature and constituent phase. Journal
455 of the Geological Society of Australia 18(1), 57-68.
- 456 Kennett, J.P., von der Borch Christopher, C., Baker Paul, A., Barton Charles, E., Boersma, A.,
457 Caulet Jean, P., Dudley Walter, C., Jr., Gardner James, V., Jenkins, D.G., Lohman William,
458 H., Martini, E., Merrill Russell, B., Morin Roger, H., Nelson Campbell, S., Robert, C.,
459 Srinivasan, M.S., Stein, R., Takeuchi, A., Blakeslee Jan, H., 1986. Site 587. Initial Reports
460 of the Deep Sea Drilling Project - Leg 90(Noumea, New Caledonia, to Wellington, New
461 Zealand, December 1982-January 1983 Part 1), 115-138.
- 462 Klingelhoefer, F., Lafoy, Y., Collot, J., Cosquer, E., Géli, L., Nouzé, H., Vially, R., 2007. Crustal
463 structure of the basin and ridge system west of New Caledonia (southwest Pacific) from
464 wide-angle and reflection seismic data. Journal of Geophysical Research - Solid Earth
465 112(B11102).
- 466 Kuramoto, S., Tamaki, K., Langseth, M.G., Nobes, D.C., Tokuyama, H., Pisciotto, K.A., Taira, A.,
467 1992. Can opalA/opalCT BSR be an indicator of the thermal structure of the Yamamoto
468 basin. Japan Sea? Proceedings of the Ocean Drilling Program, Scientific Results, 127/128.
- 469 Lafoy, Y., Géli, L., Klingelhoefer, F., Vially, R., Sichler, B., Nouzé, H., 2005. Discovery of
470 continental stretching and oceanic spreading in the Tasman sea. Eos Transactions of
471 American Geophysical Union 86(10), 101+104-105.
- 472 Lafoy, Y., Pelletier, B., Auzende, J.M., Missègue, F., Mollard, L., 1994. Tectonique compressive
473 cénozoïque sur les rides de Fairway et Lord Howe, entre Nouvelle Calédonie et Australie.

- 474 Comptes rendus de l'Académie des sciences, Série II, Sciences de la terre et des planètes
475 319, 1063-1069.
- 476 Lafoy, Y., van de Beuque, S., Missegue, F., Nercessian, A., Bernadel, G., 1998. Campagne de
477 sismique multitrace entre la marge Est Australienne et le Sud de l'arc des Nouvelles-
478 Hébrides - Rapport de la campagne RIG SEISMIC 206 (21 avril - 24 mai 1998) -
479 Programme FAUST.
- 480 Lee, G.H., Kim, H.J., Jou, H.T., Cho, H.M., 2003. Opal-A/opal-CT phase boundary inferred from
481 bottom-simulating reflectors in the southern South Korea Plateau, East Sea (Sea of Japan).
482 Geophysical Research Letters 30(24).
- 483 Lynne, B.Y., Campbell, K.A., 2004. Morphologic and mineralogic transitions from opal-A to opal-
484 CT in low-temperature siliceous sinter diagenesis, Taupo Volcanic Zone, New Zealand.
485 Journal of Sedimentary Research 74(4), 561-579.
- 486 Nobes, D.C., Murray, R.W., Kuramoto, S., Pisciotto, K.A., Holler, H., 1992. Impact of silica
487 diagenesis on physical property variations. Proceedings of the Ocean Drilling Program,
488 Scientific Results, 127/128.
- 489 Nouze, H., Henry, P., Noble, M., Martin, V., Pascal, G., 2004. Large gas hydrate accumulations on
490 the eastern Nankai Trough inferred from new high-resolution 2-D seismic data. Geophysical
491 Research Letters 31(13).
- 492 Nouzé, H., Lafoy, Y., Géli, L., Klingelhoefer, F., party, Z.c., 2005. First results of a high resolution
493 seismic study of a Bottom Simulating Reflector in the Fairway Basin, offshore New
494 Caledonia, Fifth International Conference on Gas Hydrates (ICGH 5), Trondheim, Norway.
- 495 Pecher, I.A., 2004. Waveform inversion applied to a bottom simulating reflection on the eastern
496 Lord Howe Rise. Institute of Geological and Nuclear Sciences, Science report
- 497 Ramsay, A.T.S., 1971. OCCURRENCE OF BIOGENIC SILICEOUS SEDIMENTS IN ATLANTIC
498 OCEAN. Nature 233(5315), 115-125.
- 499 Ramsay, D.C., Herzer, R.H., Barnes, P.M., 1997. Continental shelf definition in the Lord Howe Rise
500 and Norfolk Ridge regions: law of the sea survey 177, Part 1 - preliminary results.
501 Australian Geological Survey Organisation record 1997/54.
- 502 Ravenne, C., De Broin, C.E., Dupont, J., Lapouille, A., Launay, J., 1977. New Caledonia basin-
503 Fairway Ridge: structural and sedimentary study, International Symposium on Geodynamics
504 in the Southwest Pacific. Technip, Nouméa (New Caledonia), pp. 145-154.
- 505 Sultan, N., Cochonat, P., Foucher, J.P., Mienert, J., 2004. Effect of gas hydrates melting on seafloor
506 slope instability. Marine Geology 213(1-4), 379-401.
- 507 Thein, J., von Rad, U., 1987. Silica diagenesis in continental rise and slope sediments off eastern
508 North America (Sites 603 and 605, Leg 93; Sites 612 and 613, Leg 95). Initial Reports of the
509 Deep Sea Drilling Project, 95, Washington (U.S. Govt. Printing Office).
- 510 Van de Beuque, S., 2003. Geological framework of the Northern Lord Howe Rise and adjacent
511 areas. Geoscience Australia Record 2003, 1-116.
- 512 Van de Beuque, S., Auzende, J.-M., Lafoy, Y., Bernadel, G., Nercessian, A., Regnier, M., Symonds,
513 P., Exxon, N., 1998. Transect sismique continu entre l'arc des Nouvelles-Hebrides et la marge
514 orientale de l'Australie: programme FAUST (French Australian Seismic Transect). Comptes
515 Rendus de l'Académie des Sciences, Série 2 327(11), 761-768.
- 516 Volpi, V., Camerlenghi, A., Hillenbrand, C.D., Rebesco, M., Ivaldi, R., 2003. Effects of biogenic
517 silica on sediment compaction and slope stability on the Pacific margin of the Antarctic
518 Peninsula. Basin Research 15(3), 339-363.
- 519 Weissel, J.K., Hayes, D.E., 1972. Evolution of the Tasman Sea reappraised. Earth and Planetary
520 Science Letters 36, 77-84.
- 521 Williams, L.A., Crerar, D.A., 1985. SILICA DIAGENESIS - GENERAL MECHANISMS. Journal
522 of Sedimentary Petrology 55(3), 312-321.
- 523 Zelt, C.A., Smith, R.B., 1992. SEISMIC TRAVELTIME INVERSION FOR 2-D CRUSTAL
524 VELOCITY STRUCTURE. Geophysical Journal International 108(1), 16-34.
- 525

526

TABLES

527

Station	Seismic	Latitude	Longitude	Depth	BWT	Pen.	Grad T	Cond.	HF
MD06-	Correspondance	S	E	m	°C	(m)	°C/km	Wm ⁻¹ K ⁻¹	W/m ²
3022-1	Z11-11 CDP3410	23°12.11 ,	163°27.94 ,	2294	1.976	19.4	54.2 ±1.13	0.99 ± 0.04	53.82 ± 1.13
3022-2	Z11-11 CDP3410	23°12.10 ,	163°27.89 ,	2289	1.958	19.4	55.2 ±2.56		54.81 ± 2.56
3023-1	Z11-11 CDP2840	23°13.25 ,	163°29.65 ,	2344		18.4	47.4 ±1.12	1.05 ± 0.04	49.61 ± 1.12
3023-2	Z11-11 CDP2840	23°13.24 ,	163°29.65 ,	2344	1.910	18.4	46.5 ±1.11		48.66 ± 1.11
3026-1	Z11-9-2 CDP3510	23°56.26 ,	163°27.72 ,	2717	1.835	13.9	65.8 ±4.62	0.99 ± 0.03	64.40 ± 4.62
3026-2*	Z11-9-2 CDP3510	23°56.24 ,	163°27.67 ,	2717	1.8185	6.50 (bent)	77.1 ±4.09		75.46 ± 4.09
3027	Z11-9-1 CDP5701	24°40.61 ,	163°36.14 ,	2720	1.820	14.0	52.6 ±2.94	1.00 ± 0.03	52.65 ± 2.94
3028-1	Z11-9-1 CDP5015	24°45.20 ,	163°36.95 ,	2716	1.823	14.0	49.0 ±2.53	1.02 ± 0.03	49.79 ± 2.53
3028-2	Z11-9-1 CDP5015	24°45.17 ,	163°36.98 ,	2716	1.818	14.0	47.7 ±1.89		48.47 ± 1.89

528

529

530

531

532

533

534

535

Table 1 : Heat flow measurements collected during the AUSFAIR/ZoNeCo-12 after Foucher et al. (2006) in the French EEZ. Two measurements were made at each site (except MD06-3023) by multiple entry into the sediments using the PO-GO like technique. The thermal measurement at site MD06-3026-2 is not reliable, as the corer bent.

Site (MD06-)	water depth (m)	z_RN	z_RP	Z_min	Z_max
3022	2294	2862	3067	2633	2826
3023	2344	2968	3172	2727	2925
3026	2717	3292	3345	3023	3185
3027	2720	3305	3374	3090	3303
3028	2716	3030	3099	3125	3340

536

537

538

539

540

541

542

543

544

545

546

Figure captions

Figure 1: General location map of the North and Central Fairway Basin. The multichannel seismic

547 lines collected in 2004 during the ZoNeCo-11 Cruise of R/V L'Atalante are indicated in
548 red, the High Resolution Survey area being circled in blue. Yellow dots indicate heat flow
549 measurements collected in 2006 during the ZoNeCo-12 cruise of R/V Marion Dufresne.
550 The green line delineates the area surveyed in 1999 during the ZoNeco-5 cruise of R/V
551 L'Atalante.

552 Inset shows the implementation of the High Resolution Seismic lines (Z11-11 to Z11-14)
553 that were recorded during the ZoNeCo-11 cruise. The seismic signal was also recorded on
554 12 OBSs, that were deployed in 3 clusters, each cluster being composed of three OBSs
555 deployed about 500m apart from each other along the main shooting line (Z11-11) and
556 one OBS offset by about 1 km in a direction perpendicular to the main shooting line. This
557 acquisition scheme was designed to investigate the subsurface at 3 sites distinct by their
558 location with respect to the dome that affects the basement near the intersection between
559 lines Z11-11 and Z11-12: Site 1 is located away from the basement dome; Site 2 is on its
560 flank ; and Site 3 at its apex.

561

562 Figure 2: Location map of the existing seismic lines that were used in this study. Location of DSDP
563 drill hole sites is also indicated. The zoom shows the paths that were followed to track the
564 Eocene-Oligocene Unconformity from DSDP Site 208 to the High Resolution Survey
565 Area in the Fairway Basin. The northern path (Collot et al, 2008) is underlined in yellow.
566 The southern path is underlined in green (see text).

567 Figure 3: Stratigraphy at DSDP sites 206, 207 and 208 (e.g. Burns et al., 1973d; 1973c; 1973b).
568 Modified from Collot et al. (2008) Location is shown on Figure 2.

569

570 Figure 4: Zonéco 11, High Resolution line 11 (Z11-11) shot in 2004 during the ZoNeCo-11 cruise.
571 OBS locations are indicated, as well as heat flow sites (MD06-3023 and MD06-3022)
572 (after Foucher et al, 2006). Faults cutting the upper sedimentary layer are shown by
573 arrows marked with letter F. Reflectors B, C, RN and RP are described in the text.

574

575 Figure 5: Zonéco 11, High Resolution line 13 (Z11-13). F stands for « fault ». In the southwest part
576 of the section, note the strange behaviour of RN: while RN shallows, RP deepens and
577 cross-cuts sediments layers.

578

579 Figure 6: 6a) Data from OBS 02 (site 1). Direct arrivals from the seabottom are flattened with the
580 best fitting water velocity; 6b) High-resolution seismic reflection section and vertical
581 velocity profile below OBS 02, based on refraction data. Note that RN corresponds to a

582 decrease in velocity downwards, while RP is associated to an increase in velocity.

583

584 Figure 7: Seismic line 07, collected in 1999 during the ZoNeCo-5 cruise of R/V L'Atalante with a
585 6-channel streamer. After reprocessing, it clearly appears that RN corresponds to a
586 discordance. Some truncations (T) are indicated. This line is superimposed with the Z11-
587 09 profile of ZoNeCo-11. The ship tracks are such that the reflectors RN and RP that
588 were identified in the ZoNeco-11 high resolution seismic lines can be followed over the
589 Central Fairway Basin using ZoNeCo-5 lines.

590

591 Figure 8: ZoNeCo 5, line 11, showing that RN corresponds to a seismic discordance (T stands for
592 « truncations »). In the southern part (left) RN has an inverse polarity (with respect to the
593 water bottom reflection polarity). Whereas in the northern part (right) RN lies at the top
594 of a basement ridge and has a positive polarity.

595

596 Figure 9 : Sediment temperature profiles collected in 2006 during the ZoNeCo-12 cruise of R/V
597 Marion Dufresne.

598

599 Figure 10: a) zoom of the north-west part of the Z11-11 profile showing that RP divides the
600 sedimentary layers into a strong reflectivity zone (above) and a low reflectivity zone
601 (below); b) Seismic section from the Pacific margin of the Antarctic Peninsula, after (Volpi
602 et al, 2003). Note the reflectivity changes across the diagenetic BSR related to an opal-
603 A/opal-CT. Also note similarities between both sections.

Figure 1

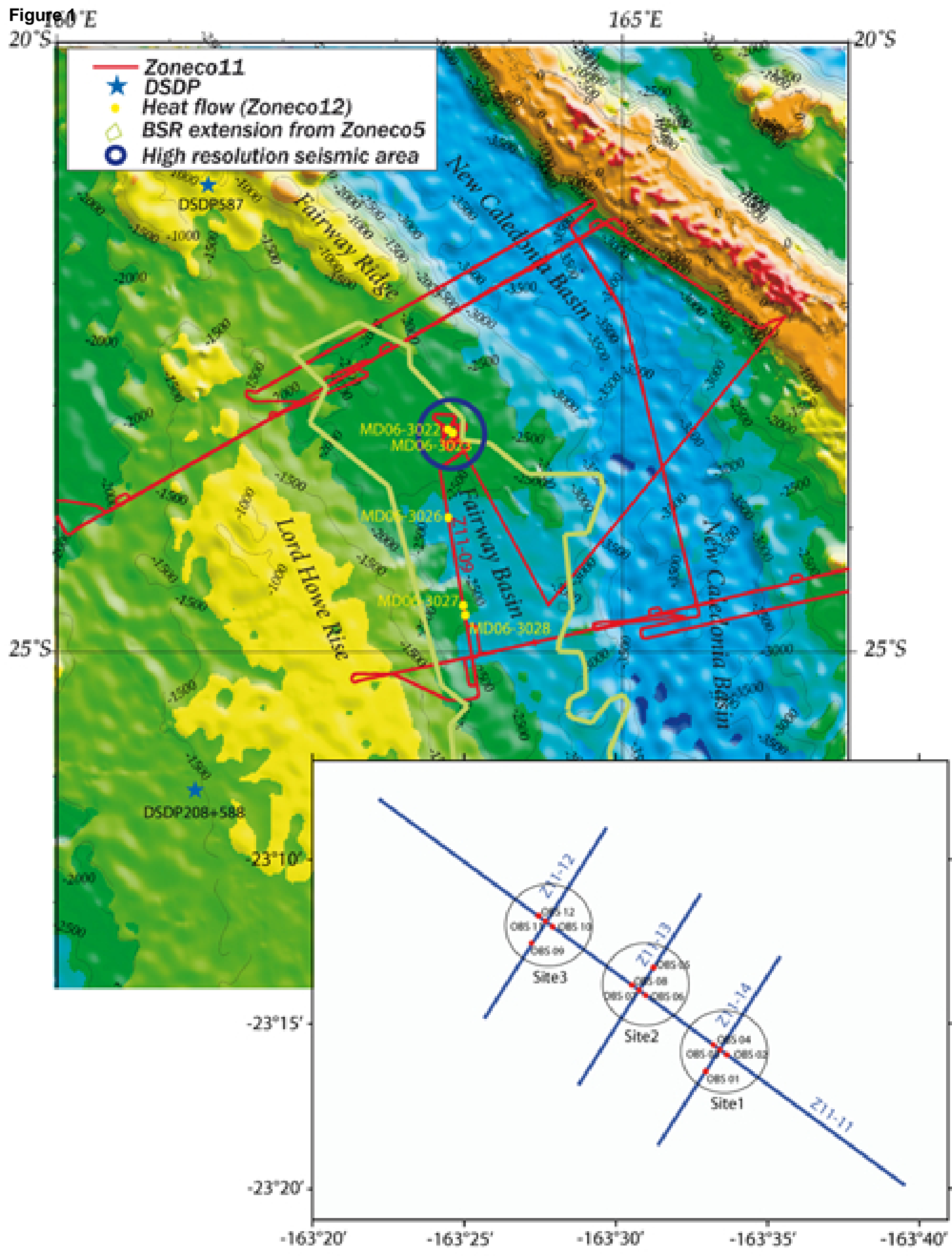


Figure 2

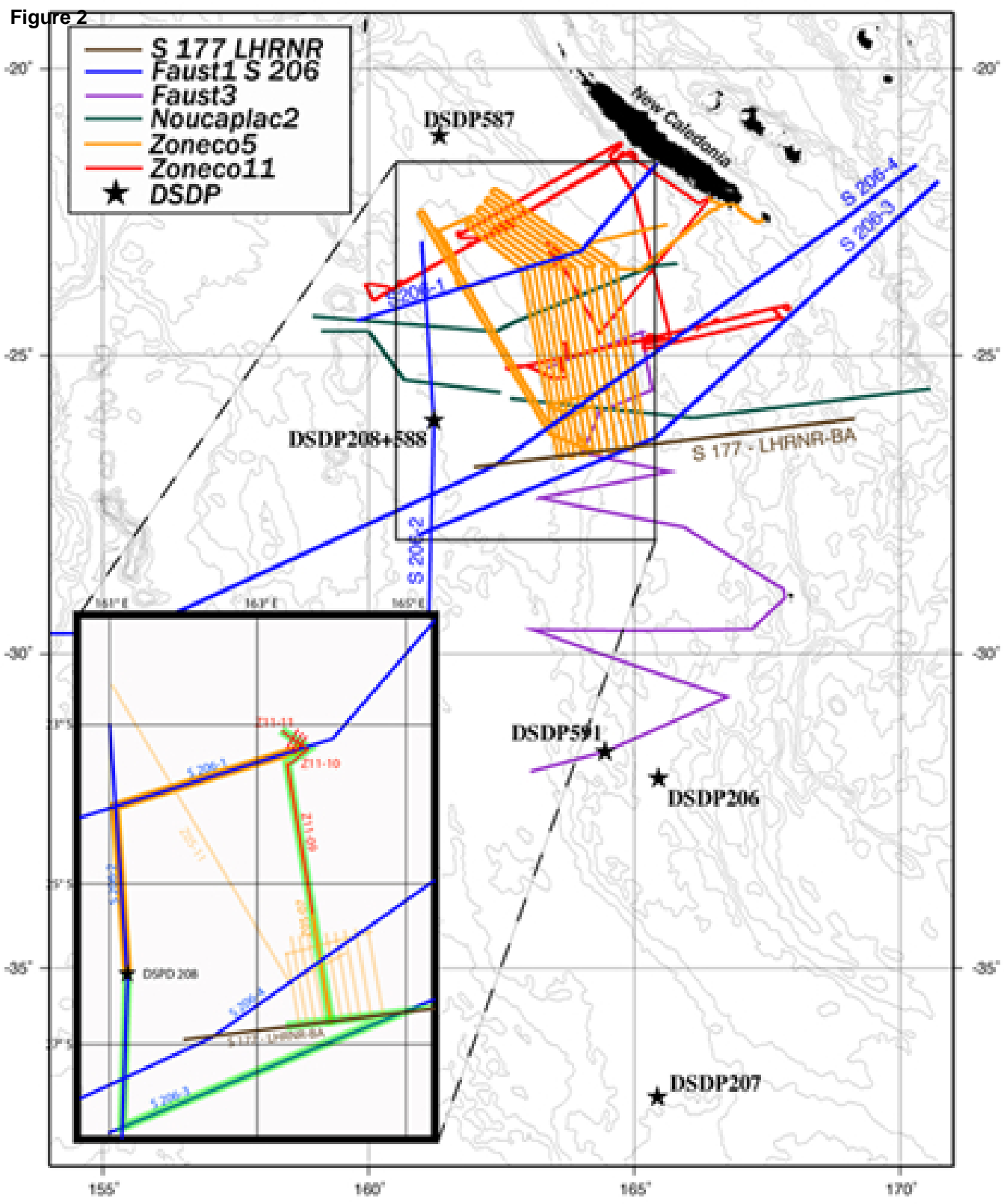


Figure 3

REGIONAL BOREHOLES

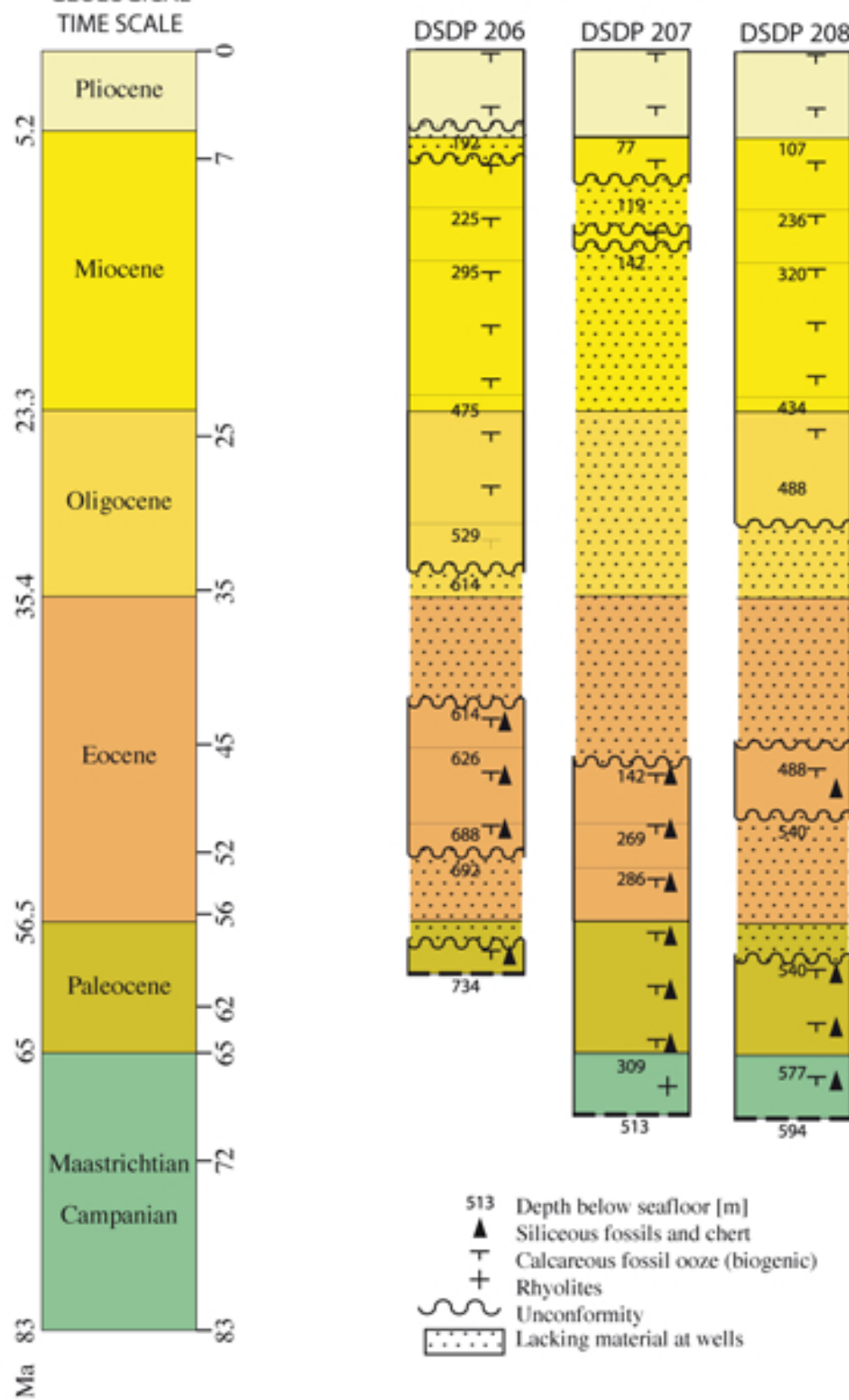


Figure 4

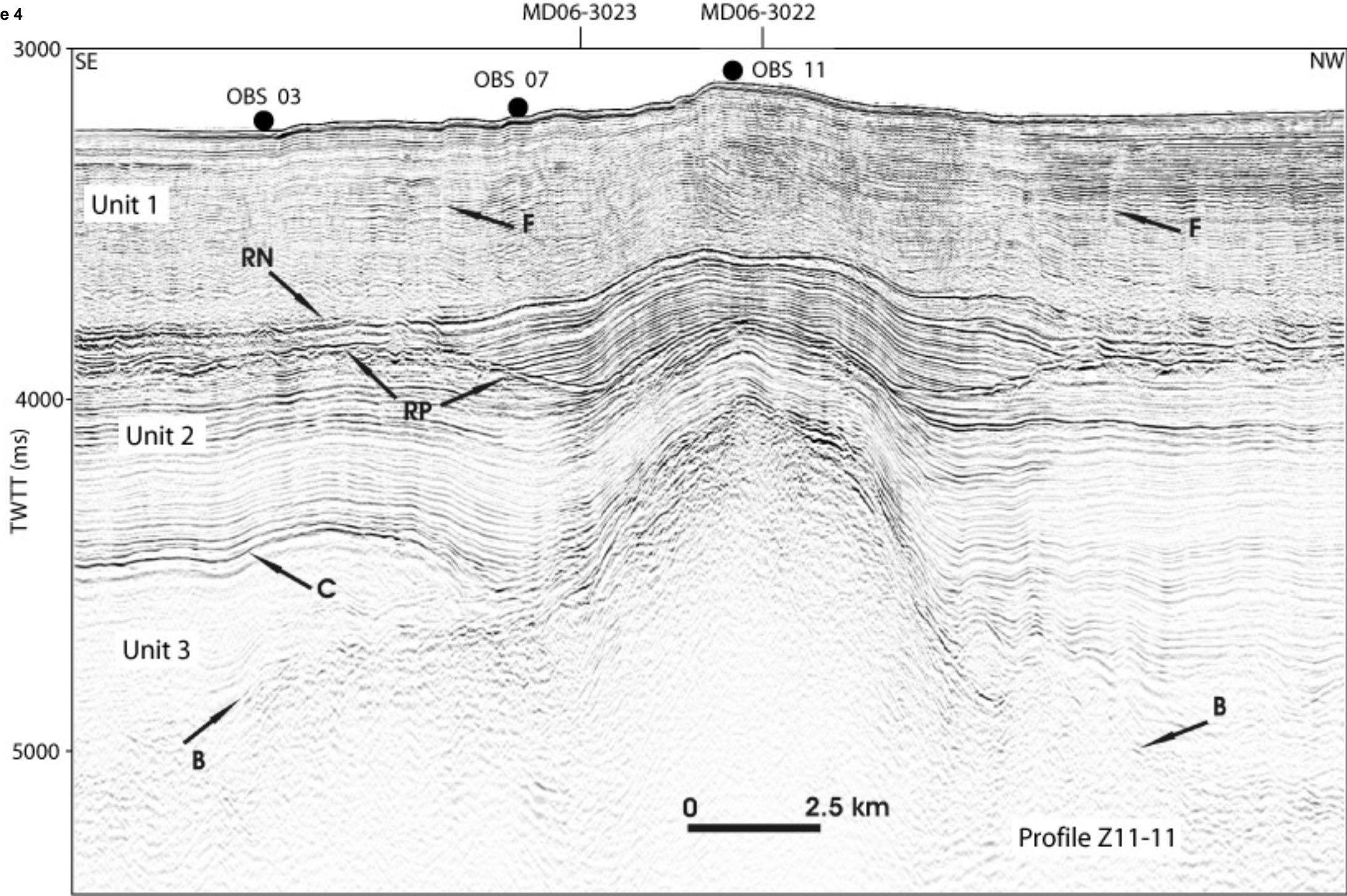


Figure 5

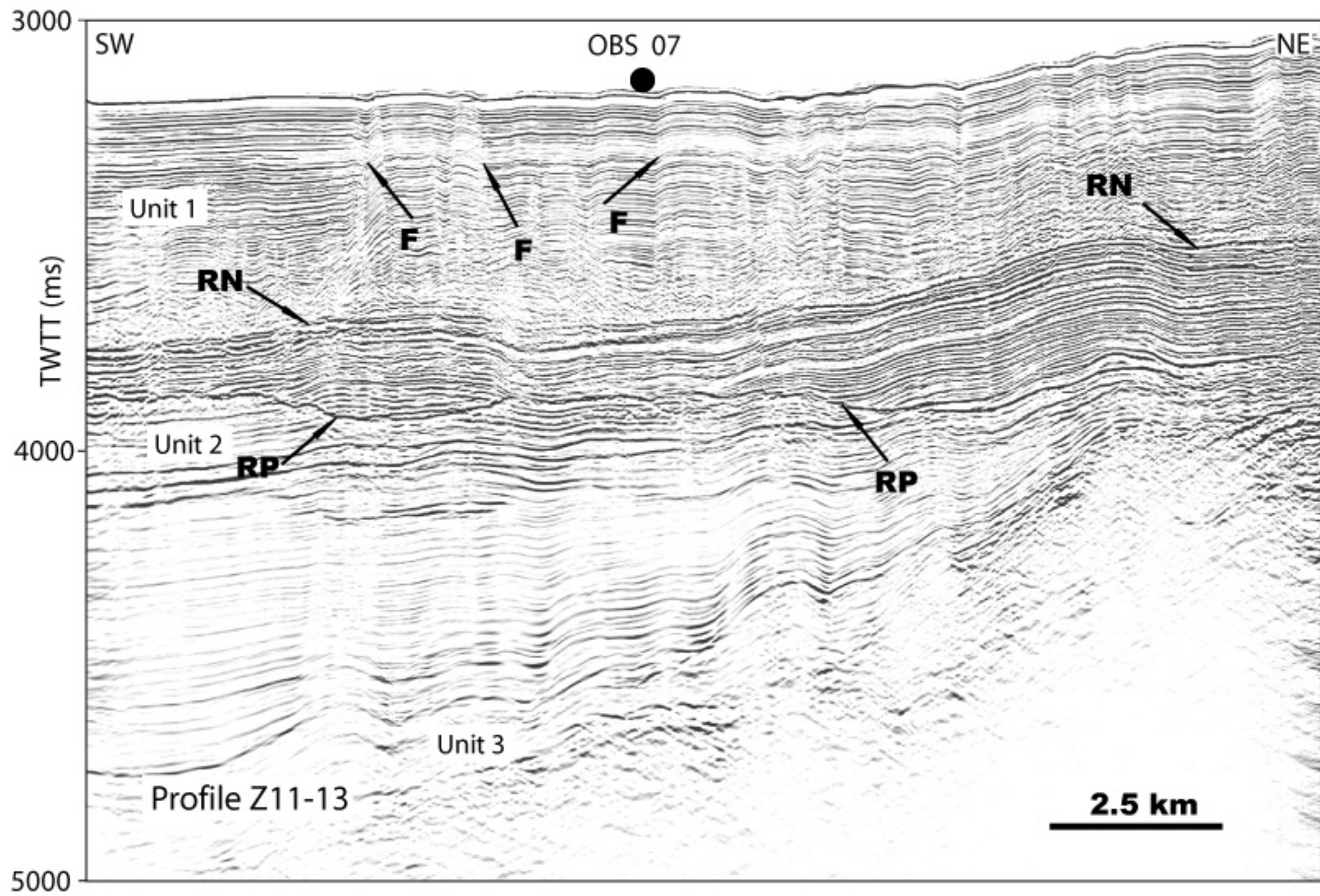


Figure 6

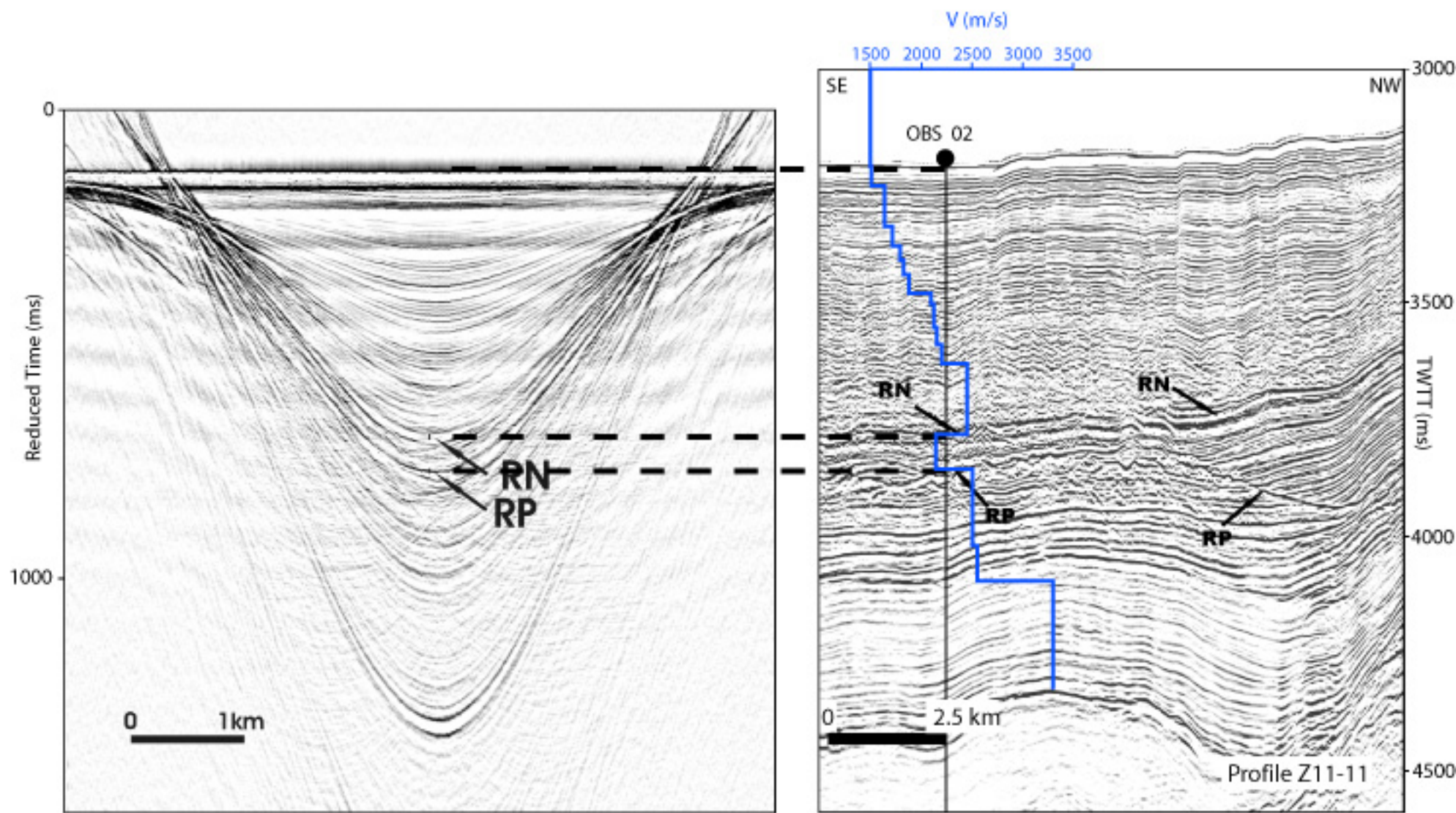


Figure 7

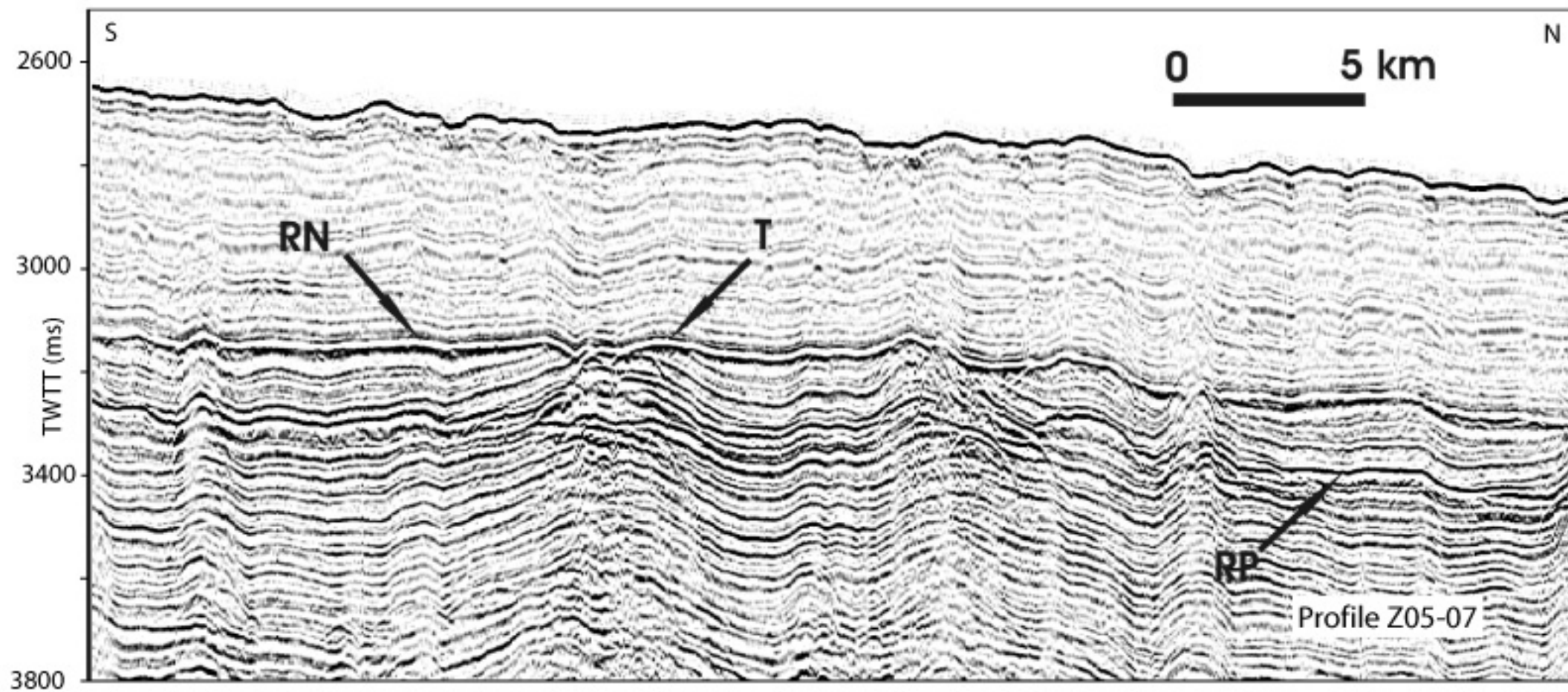
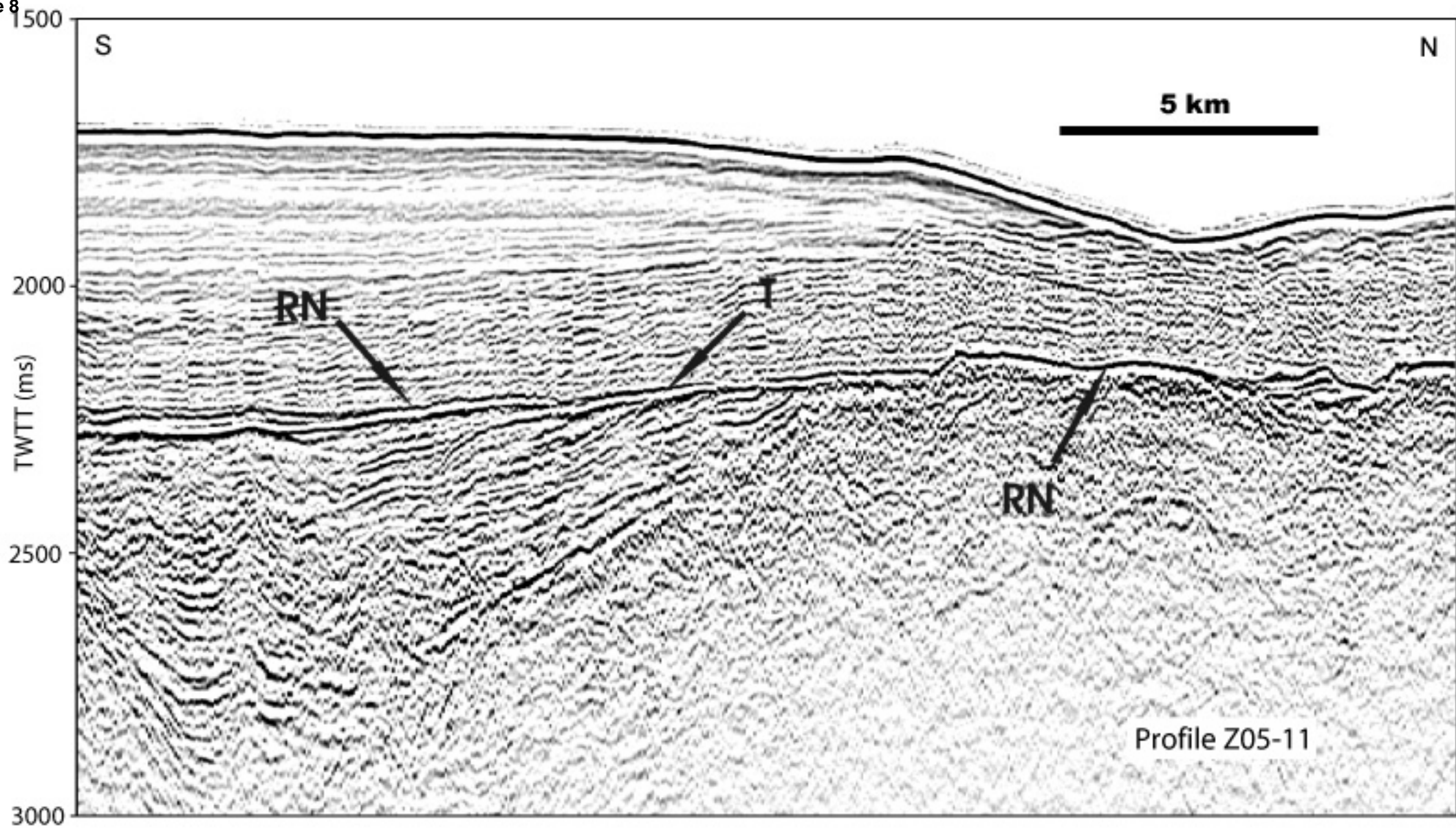


Figure 8



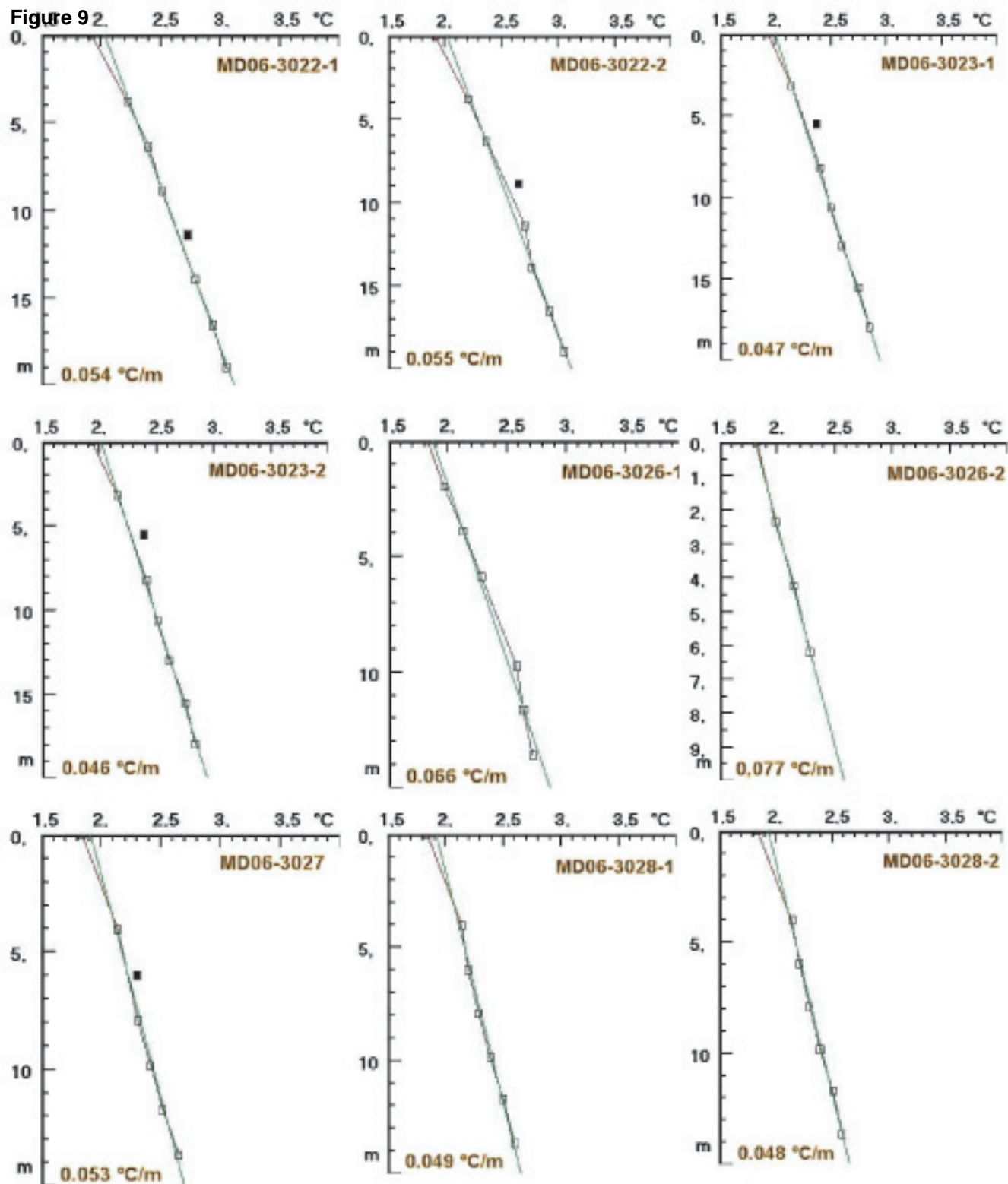


Figure 10

